IJST, Transactions of Mechanical Engineering, Vol. 37, No. M2, pp 203-215
Printed in The Islamic Republic of Iran, 2013

OPTIMIZATION OF SPECIFIC DIE PROFILES IN THIN WALLED TUBE EXTRUSION*

Z. PAHLEVANI AND R. EBRAHIMI**

Dept. of Materials Science and Engineering, School of Engineering, Shiraz University, Shiraz, I. R. of Iran
Email: ebrahimy@shirazu.ac.ir

Abstract– In the present work, three extrusion profiles have been investigated objectively, these are a conical, a cosine which is proposed in this study and a profile designed to impose equal strain increments over the equi-spaced sections. Each of them reduces a portion of the required power for extrusion. Conical profile provides the least frictional surface, cosine profile omits the surfaces of velocity discontinuity and the other profile reduces the power attributed to redundancy during deformation. However, the capability of these profiles in reducing the total power of the process is very different. Results suggest that cosine profile is the best energy-wise, whereas the profile which imposes equal strain increments over the equi-spaced sections provides the best distribution of strain in the product. In addition, a simple exponential equation as a function of die geometry is presented for the case of the profile which imposes equal strain increments over the equi-spaced sections.

Keywords– Tube extrusion, upper-bound method, finite element method, power optimization, die profile

1. INTRODUCTION

Extrusion is one of the most well known methods of forming, responsible for production of a large fraction of different profiles. Many factors should be considered when the objective is to design an extrusion die, the most important of which is the inner shape of the die and hence the geometry of the deformation zone. Conventionally, square dies are used that simply consist of two channels that come together with an abrupt change in the cross section. Despite the simplicity of these dies, they cause some problems such as generation of dead metal zones, large redundant work and non-uniform flow of metals [1]. These problems have led to many investigations to remove these shortcomings. Also, the availability of CNC machining has encouraged the investigators to develop more complicated dies which can push extrusion to the limits of ideality [2]. Talebanpour et al. proposed non-collinear channels with specific channel intersection geometries to provide a more homogenous distribution of strain and a less power consuming extrusion method [3]. A great deal of research work has been dedicated to optimizing extrusion while conserving the conventionally of collinear inlet and outlet channels. Mihelic and Stok [4] studied optimizing die profiles through mathematical techniques and finite element discretization. They proposed polynomial curves for die profile. Lin et al. [5] presented their die profile by a cubic–spline curve and used an iterative approach called updated sequential quadratic programming to accomplish the optimum calculation for unsteady metal forming based on rigid–viscoplastic finite element method. Lee et al. [6] used flexible polyhedron search method to design an optimal die profile leading to a more uniform microstructure of extruded rods. They applied their calculated profiles in experiments to verify them. Kim et al. [7] proposed a process design method to control the strain rate of the deforming material inside the

*Received by the editors October 29, 2012; Accepted April 22, 2013.
**Corresponding author

die. They used a coupled numerical approach of finite element analysis and optimization technique to provide optimum profiled die capable of inducing uniform strain rate distribution. Wifi et al. [8] implemented an incremental slab method to obtain extrusion pressure for arbitrarily curved dies. They optimized the dies considering friction at the tool-workpiece interface, strain rate, and redundant deformation. They claimed that their curved die profile produced lower stress levels than those of optimized conical die profiles.

Some investigators have shown that remarkable reduction in redundant work is achieved when streamlined flow of metal is imposed [1]. Streamlined dies are designed using different methods. Usually, mathematical expressions are fitted to build a suitable inner die surface boundary and then checked for validity by upper bound [9], genetic algorithm [10], or finite element methods [11]. In the current work, a streamlined die is proposed by a cosine expression for a thin walled tube extrusion in which the force required to perform the process is reduced with respect to other profiles. Upper bound approach and finite element simulations are used to compare the advantages of this profile with the most frequently used extrusion die profile (conical), as well as a profile providing constancy of the ratios of successive generalized homogenous strain increments (CRHS), first proposed by Blazynski [12].

2. THEORY AND CALCULATIONS

Ultra low thickness tubes with wall thicknesses of 100-400 microns are essentially produced by large reduction extrusions, thus imposing a very high amount of strain on the material. Such severely accumulated strain in the limited deformation zone of a die will in turn cause non-homogenous material flow and an extensive amount of redundant work. Furthermore, as the material passes through the micron sized opening of the die, friction gets critical because the ratio of the surface to volume of the material increases drastically. A precise die profile design seems necessary to reduce the amount of redundant work and produce more homogenous properties in the resulted tubes. Generally, for any metal forming process, the less redundant the work, the higher the quality of the product acquired and also less energy will be used for forming. Thus, the least possible amount of work should be taken into consideration in the design of die profile [12]. In the present work, objective comparison is made between three special cases of die profile, a conical die which offers the shortest frictional surface, cosine die in which the material flows in smooth streamlines with no abrupt change in its velocity, and a profile to impose a uniform accumulation of strain along the extrusion axis (CRHS die profile).

a) CRHS method

Constancy of the ratios of successive generalized homogeneous strain increments (CRHS) method is applied in design of various forming processes like tube extrusions, which results in reduction in redundancy. This method was first modeled by Blazynski [12]. As shown in Fig.1, deformation zone is divided into *n* equally spaced sections. CRHS relations are as follows [12].

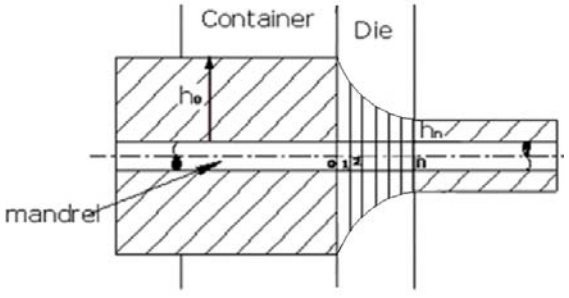

Fig.1. Deformation zone in a tube extrusion die with CRHS profile [13]

$$\frac{\varepsilon_{H2} - \varepsilon_{H1}}{\varepsilon_{H1} - \varepsilon_{H0}} = \ldots\ldots\ldots = \frac{\varepsilon_{Hn} - \varepsilon_{H(n-1)}}{\varepsilon_{H(n-1)} - \varepsilon_{H(n-2)}} = S \tag{1}$$

where ε_{Hn} is the homogeneous strain of the material passing through the 0 th to the nth section and S is a constant. This homogeneous strain is a function of the sample geometry as its diameter or wall thickness [13]. The S parameter shows the rate of deformation and can be greater, lesser, or equal to 1. If S is considered equal to 1 to ensure a constant rate of deformation, then according to Eq. (1) strain increments will be constant along the deformation zone

$$(d\varepsilon_1 = d\varepsilon_2 = d\varepsilon_3 = \ldots = d\varepsilon_n)$$

Current authors have used a simple method utilizing CRHS concept to derive the profile of the die. The proposed simple calculations are as follows.

Regarding Fig.1, homogeneous strain increment can be calculated as:

$$d\varepsilon_z = dA/A = \frac{d+2h}{h(d+h)}dh \tag{2}$$

$$d\varepsilon_\theta = -dp/p = \frac{-dh}{d+h} \tag{3}$$

$$d\varepsilon_r = -dh/h \tag{4}$$

where A is the current cross section area of the deforming sample in the deformation zone, and p is the summation of the perimeter of the current section of the profile and the perimeter of the inside hollow. d is the diameter of the mandrel and h is the current thickness of the tube. Homogeneous equivalent strain is then calculated as:

$$d\varepsilon_H = \frac{2}{\sqrt{3}}\left[\frac{3h^2+3hd+d^2}{h^2(h+d)^2}\right]^{\frac{1}{2}} dh \tag{5}$$

Regarding Eq. (5), the condition for the increments of strain to be constant over the length of the die can be formulated as Eq. (6).

$$d\varepsilon_H / dz = C \tag{6}$$

where z is collinear with the axis of extrusion, and C is a constant.

By integration of Eq. (6) over the deformation zone and using the boundary conditions $(z = z_0, h = h_f)$ the constant, C, can be determined as;

$$C = \frac{1}{z_0}\int_{h=h_0}^{h_f}\frac{2}{\sqrt{3}}\left[\frac{3h^2+3hd+d^2}{h^2(h+d)^2}\right]^{\frac{1}{2}} dh \tag{7}$$

where h_f is the final thickness of the wall.

The profile of the die is then calculated as follows:

$$z = \frac{z_0\displaystyle\int_{h=h_0}^{h}\frac{2}{\sqrt{3}}\left[\frac{3h^2+3hd+d^2}{h^2(h+d)^2}\right]^{\frac{1}{2}} dh}{\displaystyle\int_{h=h_0}^{h_f}\frac{2}{\sqrt{3}}\left[\frac{3h^2+3hd+d^2}{h^2(h+d)^2}\right]^{\frac{1}{2}} dh} \tag{8}$$

The result of which has been plotted for $0<z<7.5$ in Fig. 2.

Blazinsky [12] used a numerical method to obtain the profile resulting in constant ratios of the successive generalized homogeneous strain increments as depicted in Fig. 2, which is very close to one obtained from Eq. (8).

The latter equation can in turn be used to calculate the current thickness of the material being extruded , *h(z)*, as a function of the length of the deformation region, *L*, the radius of the mandrel, R_i, the initial outer radius of the material, R_o, and the final outer radius of the material, R_f. Due to the complexity of that equation, a simple curve fit on the points of that equation (as shown in Fig. 2) can be presented as an exponential form, which can be related to the specifications of the die to the following form:

$$h(z) = (R_0 - R_i)\exp\left(\frac{z}{L}\ln\frac{R_f - R_i}{R_0 - R_i}\right) \tag{9}$$

This equation can be used to calculate the current outer radius of the material being extruded *R(z)* too, as follows:

$$R(z) = h(z) + R_i = R_i + (R_0 - R_i)\exp\left(\frac{z}{L}\ln\frac{R_f - R_i}{R_0 - R_i}\right) \tag{10}$$

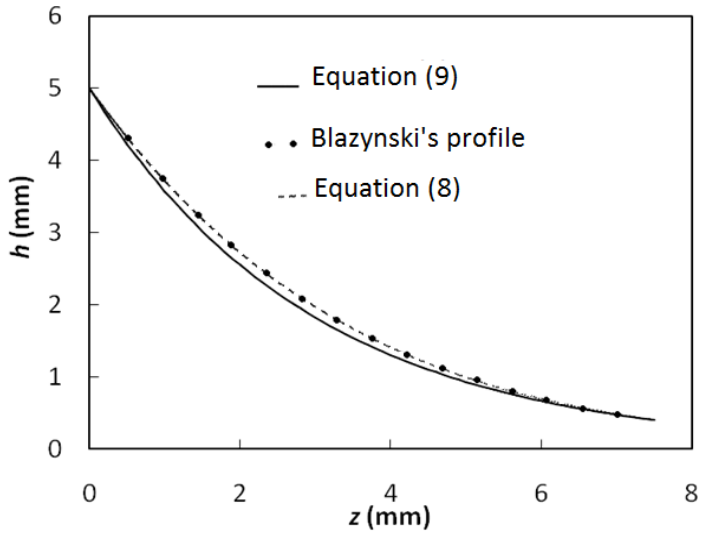

Fig. 2. The die profile calculated by CRHS method

Homogeneity of the distribution of straining over the deformation region results in a better flow of the material, thus reducing the redundant work during deformation.

b) Upper bound calculations for tube extrusion through curved die profiles

An upper-bound method proposed by Chang and Choi [14] is implemented to calculate the power dissipation in the curved die profiles. As it can be seen in Fig. 3, deformation takes place at region II; Γ1 and Γ2 are the velocity discontinuity surfaces, and Γ3, Γ4 are frictional surfaces. The profile is a function of *z* and is designated as *R*(*z*).

.

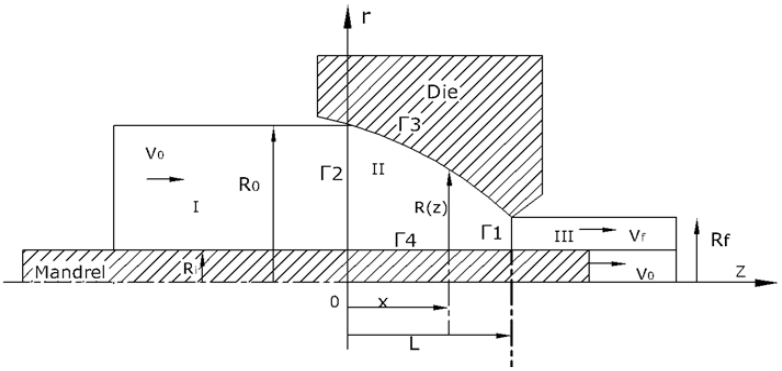

Fig. 3. Geometrical parameters in a curved die profile [14]

The velocity of the material before entering the deformation region is v_0, thus the horizontal velocity of the material in the deformation zone can be obtained regarding incompressibility of the material as:

$$v_z = \frac{R_0{}^2 - R_i{}^2}{R(z)^2 - R_i{}^2} v_0 \tag{11}$$

The radial component of the velocity is proposed to be [14]:

$$v_r = \frac{R(z)R'(z)(R_0{}^2 - R_i{}^2)(r^2 - R_i{}^2)v_0}{r(R(z)^2 - R_i{}^2)^2} \tag{12}$$

Considering the axisymmetric nature of the process, the circumferential component of the velocity (v_θ) is equal to zero. Differentiating the velocity field with respect to coordinates results in the strain rate field:

$$\begin{aligned}
&\dot{\varepsilon}_{rr} = \frac{\partial v_r}{\partial r} = \frac{R(z)R'(z)(R_0{}^2 - R_i{}^2)(r^2 + R_i{}^2)v_0}{r^2(R(z)^2 - R_i{}^2)^2} \\
&\dot{\varepsilon}_{\theta\theta} = \frac{v_r}{r} + \frac{1}{r}\frac{\partial v_\theta}{\partial \theta} = \frac{R(z)R'(z)(R_0{}^2 - R_i{}^2)(r^2 - R_i{}^2)v_0}{r^2(R(z)^2 - R_i{}^2)^2} \\
&\dot{\varepsilon}_{zz} = \frac{\partial v_z}{\partial z} = \frac{-2R(z)R'(z)(R_0{}^2 - R_i{}^2)v_0}{(R(z)^2 - R_i{}^2)^2} \\
&\dot{\varepsilon}_{r\theta} = \dot{\varepsilon}_{\theta z} = 0 \\
&\dot{\varepsilon}_{rz} = \frac{1}{2}\left(\frac{\partial \dot{v} r}{\partial z} + \frac{\partial v_z}{\partial r}\right) = \\
&\frac{(R_0{}^2 - R_i{}^2)(r^2 - R_i{}^2)\{R(z)R''(z)(R(z)^2 - R_i{}^2) - R'(z)^2(3R(z)^2 + R_i{}^2)\}v_0}{2r(R(z)^2 - R_i{}^2)^3}
\end{aligned} \tag{13}$$

As it can be seen, the necessary condition of volume constancy is satisfied ($\dot{\varepsilon}_{rr} + \dot{\varepsilon}_{\theta\theta} + \dot{\varepsilon}_{zz} = 0$).
Upper-bound theorem assumes the total power required to carry out a process to be spent for deformation, crossing the surfaces of velocity discontinuity, overcoming friction, and occasionally displacing the external tractions on the material.

$$\dot{W}_{tot} = 2k \int_V \sqrt{\frac{1}{2}\dot{\varepsilon}_{ij}\dot{\varepsilon}_{ij}}\, dV + \int_{S_\Gamma} k\left|\Delta v_\Gamma\right| dS + \int_{S_f} mk\left|\Delta v_f\right| dS - \int_{Si} T_i v_i dS \tag{14}$$

where k is the mean shear yield stress of the material and m is the constant friction factor. s_Γ, s_f and s_i stand for the areas of velocity discontinuity surfaces, frictional surfaces and traction surfaces respectively.

Based on the results of the compression test at room temperature, the Holloman's equation for the material used in this study was obtained as: $\sigma = 106\varepsilon^{0.349}\ MPa$. Therefore, the mean shear yield stress which is related to the mean flow stress, $\overline{\sigma}$, can be calculated ($k = \frac{\overline{\sigma}}{\sqrt{3}}$).

The differential volume element considered for the deformation zone aimed at calculating the first integral is:

$$dV = 2\pi r dr dz \tag{15}$$

in which z varies from *0* to *L* and *r* from R_i to $R(z)$.
Thus the first integral of Eq. (14) will be calculated as:

$$\dot{W}_i = \left| \frac{4\pi\overline{\sigma}}{\sqrt{3}} \int_0^L dz \int_{R_i}^{R(z)} dr \frac{(R_0^{\,2} - R_i^{\,2})}{r(R(z)^2 - R_i^{\,2})^2} \sqrt{R(z)^2 R'(z)^2 (3r^4 + R_i^{\,4}) + \frac{(r^2 - R_i^{\,2})^2 r^2 F(z)^2}{4(R(z)^2 - R_i^{\,2})^2}} \right| v_0 \tag{16}$$

in which $F(z) = R(z)R''(z)(R(z)^2 - R_i^2) - R'(z)^2(3R(z)^{\,2} + R_i^2)$.

The differential surface element for calculation of the second integral is considered to be:

$$ds = 2\pi r dr \tag{17}$$

The velocity discontinuities on Γ_1 and Γ_2 surfaces are:

$$\Delta v_2 = \frac{R_0 |R'(0)|(r^2 - R_i^{\,2})}{r(R_0^{\,2} - R_i^{\,2})} v_0$$
$$\Delta v_1 = \frac{R_f |R'(L)|(R_0^{\,2} - R_i^{\,2})(r^2 - R_i^{\,2})}{r(R_f^{\,2} - R_i^{\,2})} v_0 \tag{18}$$

Thus the second integral Eq. (14) is calculated as:

$$\dot{W}_{s_1} = \int_{S_{\Gamma_1}} \tau_1 . \Delta v_1 . ds = \left| \frac{2\pi\overline{\sigma}\ R_f . R'(L)(R_0^{\,2} - R_i^{\,2})}{3\sqrt{3}(R_f^{\,2} - R_i^{\,2})^2} . (R_f^{\,3} - 3R_f R_i^{\,2} + 2R_i^{\,3}) \right| v_0$$
$$\dot{W}_{s_2} = \int_{S_{\Gamma_2}} \tau_2 . \Delta v_2 . ds = \left| \frac{2\pi\overline{\sigma} R_0 . R'(0)}{3\sqrt{3}(R_0^{\,2} - R_i^{\,2})^2} . (R_0^{\,3} - 3R_0 R_i^{\,2} + 2R_i^{\,3}) \right| v_0 \tag{19}$$

The differential surface elements for the frictional surfaces Γ_3 and Γ_4 are:

$$ds = 2\pi R(z)\sqrt{1 + R'(z)} dz \tag{20}$$

$$ds = 2\pi R_i dz \tag{21}$$

and the corresponding velocity discontinuities are:

$$\Delta v_3 = \left| \frac{(R_0^{\,2} - R_i^{\,2})}{R(z)^2 - R_i^{\,2}} . \sqrt{1 + R'(z)^2} \right| v_0$$
$$\Delta v_4 = \left| \frac{R_0^{\,2} - R(z)^2}{R(z)^2 - R_i^{\,2}} \right| v_0 \tag{22}$$

The third integral Eq. (14) can then be calculated as:

$$\dot{W}_{s_3} = \int_{S_{\Gamma_3}} \tau_3 . \Delta v_3 . ds = \left| \frac{2\pi\bar{\sigma}\, m(R_0{}^2 - R_i{}^2)}{\sqrt{3}} . \int_0^L \frac{R(z)}{R(z)^2 - R_i{}^2} (1 + R'(z)^2) dz \right| v_0$$

$$\dot{W}_{s4} = \int_{S_{\Gamma_4}} \tau_4 . \Delta v_4 . ds = \left| \frac{2\pi\bar{\sigma}\, mR_i}{\sqrt{3}} . \int_0^L \frac{R_0{}^2 - R(z)^2}{R(z)^2 - R_i{}^2} dz \right| v_0 \tag{23}$$

The total power supplied by the external source to perform the process at a constant speed is the product of the force times the speed of the ram. The relative pressure of the extrusion can then be obtained:

$$\dot{W}_{tot} = Fv_0 = P_{Extrusion}\ \pi(R_0{}^2 - R_i{}^2)\ v_0$$
$$\frac{P_{Extrusion}}{\bar{\sigma}} = \frac{\dot{W}_{tot}}{v_0 \bar{\sigma} \pi (R_0{}^2 - R_i{}^2)} \tag{24}$$

As it can be seen from Eq. (24), the geometry of the deformation zone can affect all three sources of power consumption. An inappropriate die profile can cause abrupt changes in the material velocity, making the flow inhomogeneous and producing redundant work. Moreover, the total length and the perpendicular pressure on the frictional surfaces are closely related to the geometry of the die profile. Friction can by itself alter the imposed strain on the material as well as raise the required forces for performing the process.

c) Cosine die profile

The more gradual the straining of the material is, the less power needed for the deformation portion of the total power. However, existence of the velocity discontinuity surfaces results in consumption of some unnecessary power (Fig. 3). If the die profile is designed to omit these surfaces and the material enters and exits the deformation zones with no abrupt change in its velocity vector, a considerable amount of power will be saved.

As can be deduced from Eq. (19), velocity discontinuities on the Γ_1 and Γ_2 surfaces depend on the slope of the profile at the corresponding points. In the case of cosine profile, the slope at these points is zero and there is no velocity discontinuity. The general form of a cosine die profile can be considered as:

$$R(z) = \frac{R_0 + R_f}{2} + \frac{R_0 - R_f}{2} Cos\left(\frac{\pi z}{L}\right) \tag{25}$$

Satisfying the boundary conditions $z = 0 \rightarrow R = R_0$ and $z = L \rightarrow R = R_f$.

d) Extrusion through specific die profiles

Three die profiles are compared; a conical profile, a profile obtained from CRHS method, and a cosine die profile. The profiles for each case are:

$$\text{Cosine profile: } R(z) = \frac{R_0 + R_f}{2} + \frac{R_0 - R_f}{2} Cos\left(\frac{\pi z}{L}\right) \tag{26}$$

$$\text{CRHS profile: } R(z) = R_i + (R_0 - R_i)\exp\left(\frac{z}{L}\ln\frac{R_f - R_i}{R_0 - R_i}\right) \tag{27}$$

$$\text{Conical Profile: } R(z) = \frac{R_f - R_0}{L} z + R_0 \tag{28}$$

Power dissipation is calculated for each case considering the same deformation condition. For each case two reductions in area are assumed; first, a 95.7% reduction in area (an initial tube of 7.5 mm in outer radius and 2.5 mm in inner radius is turned into a tube of 2.5 mm in inner radius but only a wall thickness of 400 microns.), and second, a 60% reduction in area (an initial tube of 7.5 mm in outer radius and 2.5 mm in inner radius is turned into a tube of 2.5 mm in inner radius and a wall thickness of 2.6 mm). Numerical method was implemented to calculate the integrals since there are no simple forms for them to be calculated analytically.

Strain distribution is evaluated in the deformation zone for each of the three cases and each of the two reductions in area. Equation (5) shows the increments of equivalent homogeneous strain in tube extrusion. *h* is the current thickness of the tube in the deformation zone and it can be written as $R(z) - R_i$. Thus, *dh* as well as strain increment can be formulated as a function of *z*:

$$dh = R'(z)dz \tag{29}$$

$$\varepsilon_H(z) = \int_0^z \frac{2}{\sqrt{3}}\left[\frac{3(R(z)-R_i)^2 + 3(R(z)-R_i)d + d^2}{(R(z)-R_i)^2((R(z)-R_i)+d)^2}\right]^{\frac{1}{2}} R'(z)dz \tag{30}$$

Strain is then plotted as a function of z, and the variations of dissipated power through z are investigated.

e) Numerical evaluations

Numerical simulations were implemented using commercial finite element code, DEFORM-2D, to verify the results of analytical calculation. The three profiles were modeled utilizing their axisymmetric geometry. A total number of 8000 square mesh elements were used for each case and the plastic flow and frictional behavior of the material obtained from compression test ($\sigma = 106\varepsilon^{0.349}\ MPa$ and $\mu = 0.038$) was inserted to the software. A length of 7.5 mm was used for the simulations that, for an initial outer radius of the material produces a nearly optimized deformation process for all the cases, which will be discussed later.

3. RESULTS AND DISCUSSION

a) Strain accumulation

Figure 4 shows the accumulation of homogeneous strain for the different profiles and reductions in area. It is noted that normalized distance is the ratio of *z* to the length of deformation zone (*L*) and accumulated strain is the total homogeneous strain that material has experienced at every distance of deformation zone.

The amount of homogenous strain is only a function of the initial and final areas and for all the cases with 95.7% reduction in area is 3.45. However, as it can be seen and was expected, the variation of strain with the length that the material has gone through the deformation zone is linear for CRHS profile and shows the most uniform accumulation of strain in this profile. For severe reductions in area, the deviation of strain accumulations for conical and cosine dies are more pronounced with respect to CHRS die, indicating that for higher amounts of reductions in area, the shape of the profile will more rigorously affect the accumulation of strain.

d) Optimized die profile for tube extrusion

Consumed power due to internal deformation, velocity discontinuities and frictional surfaces are calculated for each of the three cases and each of the two reductions in area. According to Fig. 5, total power dissipation at the end of the process is minimum for cosine die profile.

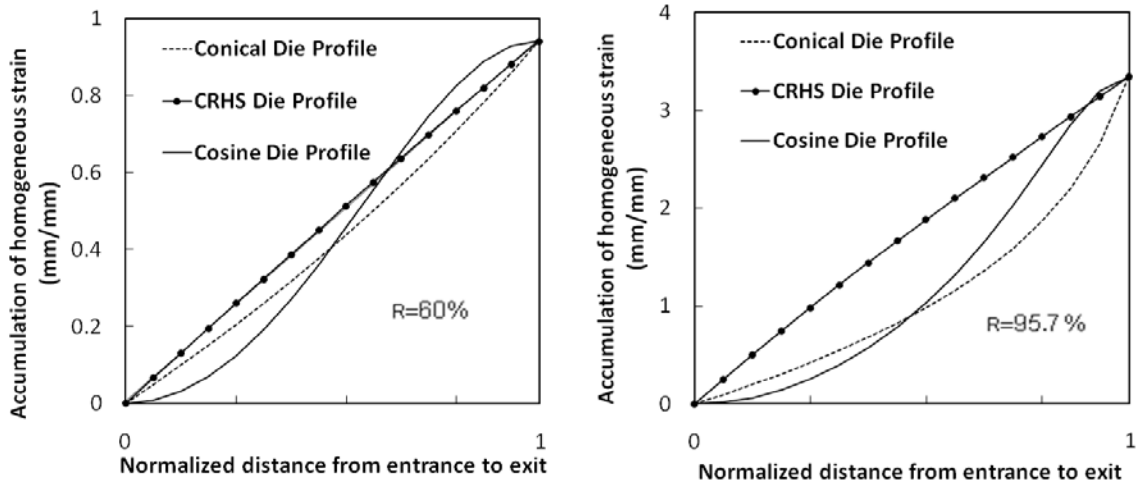

Fig. 4. Accumulation of homogenous strain during deformation, for 60% and 95.7% reductions in area

The power dissipation due to velocity discontinuity for cosine profile is equal to zero, since the material enters and exits the deformation zone tangent to the streamlines of the deformation zone. The largest dissipation occurs for CRHS profile which gets larger as the reduction in area increases. The difference between conical die and CRHS profile rises with increasing reduction in area. Based on the calculation of power consumption for the first integral of Eq. (14) as internal deformation power, the least amount is consumed in CRHS profile. This is consistent with the fact that CRHS profile provides the most uniform and gradual strain accumulation and thus the least non-homogeneous deformation, which leads to lesser internal power consumption. It can be deduced that any increase in inhomogeneity of straining will cause more internal power dissipation for the process. As severe reductions in area result in generation of redundancy and inhomogeneous flow of the material, careful design of the style of accumulating strain can effectively reduce the required power. However, at low reductions in area, the differences between CRHS and the other profiles subside. Power dissipated on frictional surfaces depends on the length of the frictional surfaces as well as the normal pressure on these surfaces. The consumed power due to friction rises from the least amount for conical profile to the highest amount for CRHS method.

Figure 5 shows the total consumed power during deformation. The end point of the diagrams show the sum of total consumed power for each profile. As depicted, this power is lowest for cosine profile, which is resulted from omission of the velocity discontinuities. As mentioned before, all the integrals for calculation of the powers are performed on the deformation zone from entrance to exit of the die to show the power consumption during deformation.

Figure 6 shows the calculated relative extrusion pressure as a function of the normalized length of the dies for 60% and 95.7% reductions in area. According to this figure, the optimized relative die lengths for a 95.7% reduction in area are 1.2 for cosine, 1.3 for conical, and 1.06 for CRHS profiles. These quantities for a 60% reduction in area are 1.13, 1.19, and 1.13, respectively. In the case of 95.7% reduction in area, for relative die lengths less than 1.2, the minimum relative extrusion pressure corresponds to cosine profile. This is due to the omission of velocity discontinuities in this profile. Beyond this point, cosine profile crosses higher than conical die which is because of the rise in frictional power dissipation due to much longer frictional length of the die in cosine profile. In contrast, in the case of 60% reduction in area, for all values of relative die lengths, cosine profile offers the minimum required energy. In this case, due to the lower amount of reduction in area, the power required to overcome friction cannot outweigh the reduction in the power due to the omission of the velocity discontinuities.

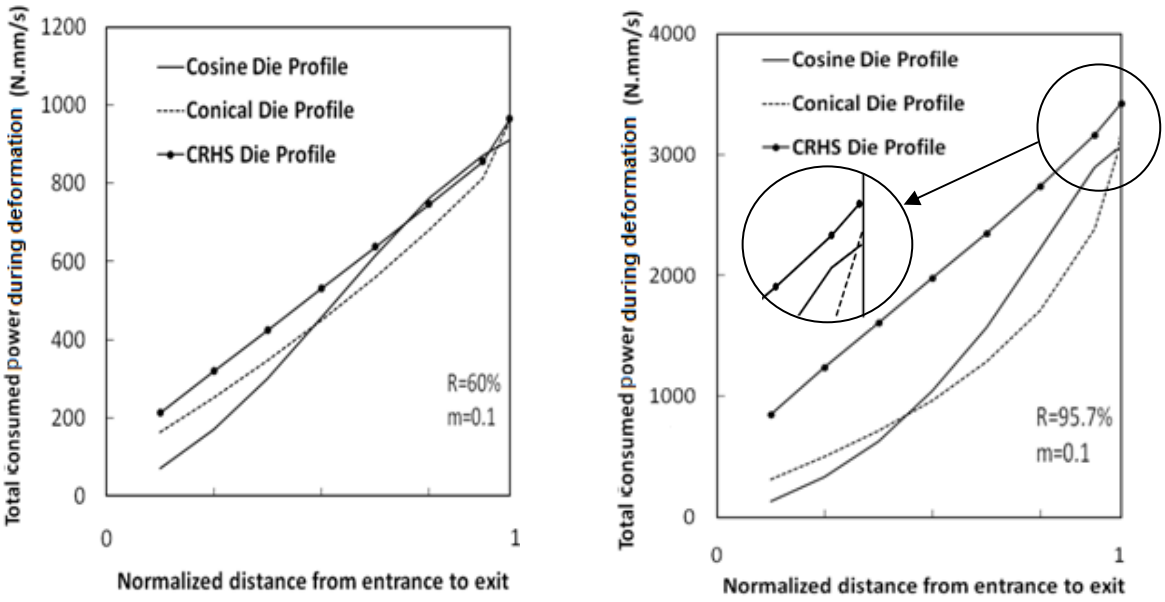

Fig. 5. Total power dissipation during deformation for 60% and 95.7% reductions in area

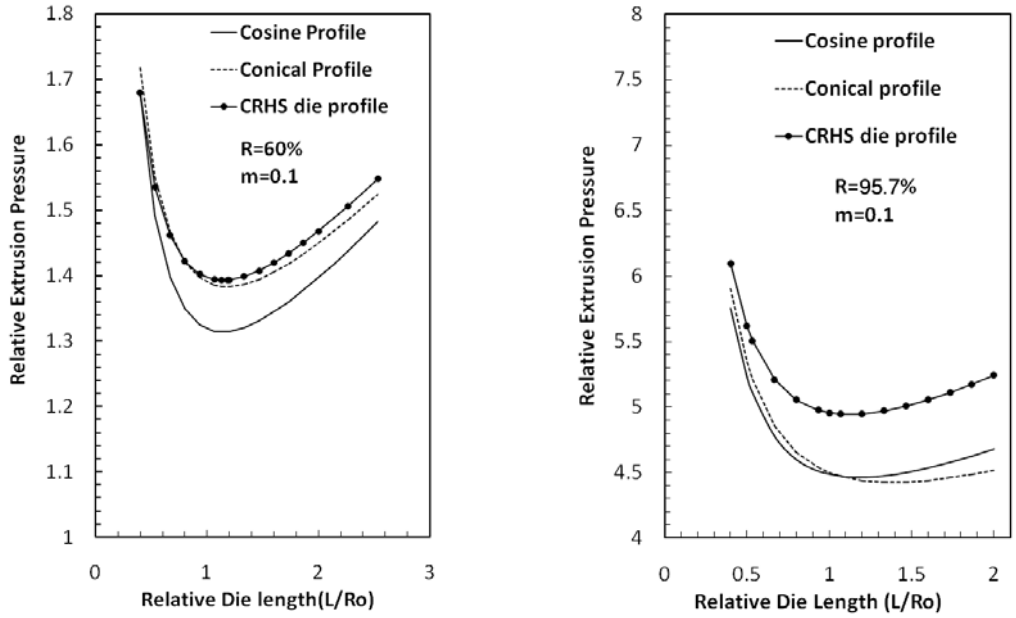

Fig. 6. Relative extrusion pressure versus relative die length for different die profiles and two reductions in area

c) Finite element simulation

Figure 7 shows the strain contours for each of the three profiles. As seen, CRHS profile offers the most homogenous distribution of strain, the least amount of total strain with respect to the other two profiles and also straining takes place over the entire length of the profile. On the other side, conical profile can be considered as the worst case, in which straining begins much sooner for the material adjacent to the wall of the die, and there it gives the largest amount of total strain. These observations are consistent with the design factors of each die. CRHS profile was designed to provide a gradual and uniform straining over the length of the die and thus to minimize the amount of redundant strain during deformation. Therefore, occurrence of the least total strain and a uniform distribution of strain were expected.

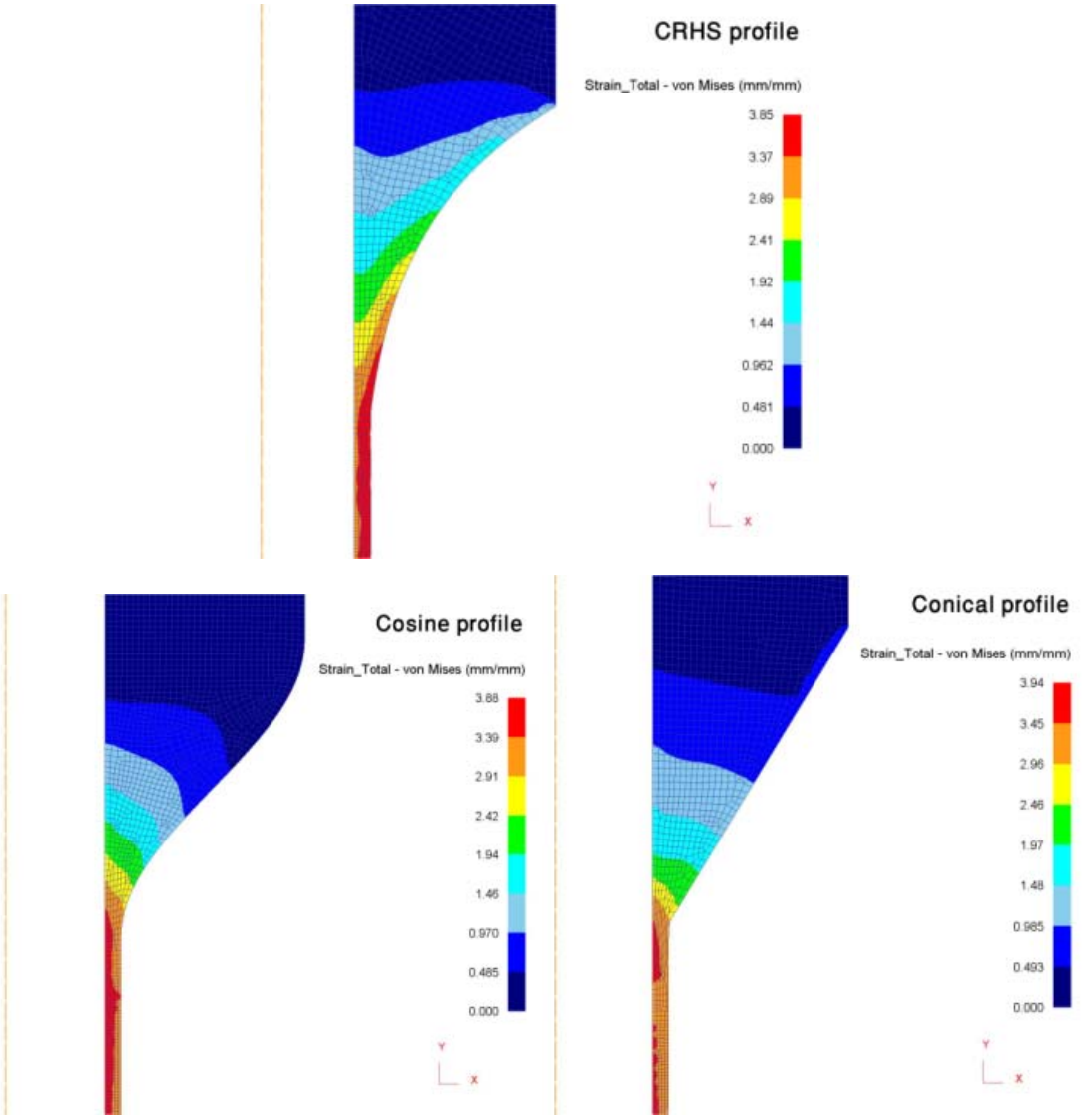

Fig. 7. Color strain contours showing the distribution of strain in the three profiles

Figure 8 shows the force for each process as a function of the punch stroke according to FEM and upper-bound solution. Cosine profile offers the least amount of the punch force. This is in total agreement with the upper-bound results. Regarding cosine profile, there is no surface of velocity discontinuity and so no power dissipated by the material to pass through it. Consequently, the total power and the required force for the process is the minimum**.** As discussed before, the minimum total strain and also the minimum internal deformation power consumption occurred in CRHS profile but the total power consumption and force is higher in CRHS profile compared with the two other profiles. Accordingly, it could be said that CRHS profile reduces only the internal power consumption, not the total power. But Cosine profile reduces the total power consumption by elimination of discontinuity surfaces.

The differences in calculated force for extrusion between two solution methods are about 10 %. The difference in predicted force between cosine and conical profile is as small as 0.6 kN, which is in total agreement with the slight difference in punch force for cosine and conical profile according to FEM results (Fig. 8). It is emphasized that a small increase in load prediction by the theory is due to the nature of upper-bound method which over estimates the required load. Figure 8 also shows local peaks for CRHS and conical profiles, these peaks can be attributed to the sudden change in flow direction of materials entering deformation zone.

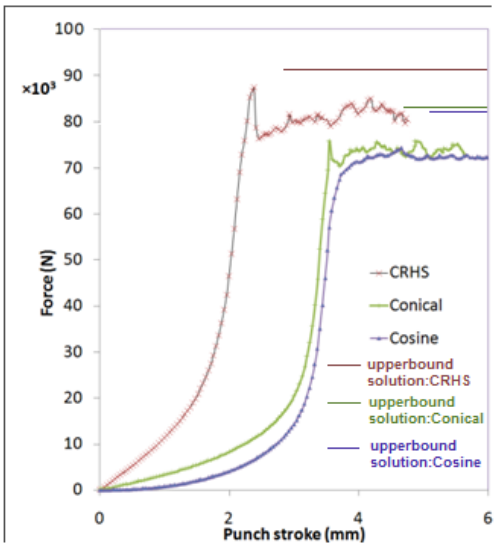

Fig. 8. The extrusion force versus punch stroke curves

4. CONCLUSION

Analytical calculations and finite element simulations for the three proposed profiles of tube extrusion were in good agreement and confirm that:

1- Cosine profile offers the best energy wise efficiency for tube extrusion. In this profile, the extended contact length of the profile is compromised by the omission of any power consuming velocity discontinuity surface.

2- CRHS profile is designed to uniformly accumulate strain over the length of the die. The homogenously distributed strain in CRHS profile generates the least amount of redundant strain during deformation and thus the least amount of the total strain.

3- Straining begins immediately as the material enters CRHS profile, providing a very gradual deformation of the material over the whole length of the die. However, for the cosine profile the material travels a finite length inside the profile before bearing a considerable amount of strain. For the case of conical die, straining begins markedly sooner for the material adjacent to the wall of the profile causing a gradient of strain across the cross section of the material which is retained to the end of the process.

4- For the case of CRHS profile, a simple exponential equation is presented as a function of die geometry.

REFERENCES

1. Narayanasamy, R., Srinivasan, P. & Venkatesan, R. (2003). Computer aided design and manufacture of streamlined extrusion dies. *Journal of Materials Processing Technology*, Vol. 138, pp. 262–264.
2. Avitzur, B. (1968). *Metal forming processes and analysis*. Mc Graw Hill, New York, 1968.
3. Talebanpour, B., Pardis, N., Hariri, M. & Moshksar, M. M. (2010). Utilization of channel angular deformation as an alternative for direct extrusion. *Materials Science and Engineering*: *A*, Vol. 527, pp. 2492-2497
4. Mihelic, A. & Stok, B. (1998). Tool design optimization in extrusion process. *Computers & Structures*, Vol. 68, pp. 283-293.
5. Zou Lin, Xia Juchen, Wang Xinyun, Hu Guoan, (2003). Optimization of die profile for improving die life in the hot extrusion process. *Journal of Materials Processing Technology*, Vol. 142, pp. 659–664.

6. Lee, S. K., Koo, D. C. & Kim, B. M. (2000). Optimal die profile design for uniform microstructure in hot extrusion. *International Journal of Machine Tools and Manufacture*, Vol. 40, pp. 1457-1478.
7. Kim, N. H., Kange, C. G. & Kim, B. M. (2001). Die design optimization for axisymmetric hot extrusion of metal matrix composites. *International Journal of Mechanical Sciences*, Vol. 43, pp. 1507-1520.
8. Wifi, A. S., Shatla, M. N. & Abdel Hamid, A. (1998). An optimal-curved die profile for hot rod extrusion process. *Journal of Materials Processing Technology*, Vol. 73, pp. 97-107.
9. Narayanasamy, R., Ponalagusamy, R., Venkatesan, R. & Srinivasan, P. (2006). An upper bound solution to extrusion of circular billet to circular shape through cosine dies. *Journal of* Materials & Design, Vol. 27, pp. 411–415.
10. Chung, J. S. & Hwary, S. M. (1997). Application of genetic algorithm to the optimal design of the die shape in extrusion. *Journal of Materials Processing Technology*, Vol. 72, pp. 69–77.
11. Venkata Reddy, N., Sethuraman, R. & Lal, G. K. (1996). Upper bound and finite element analysis of axisymmetric hot extrusion, *Journal of Materials Processing Technology,* Vol. 57, pp. 14–22.
12. blazynski, T. Z. (1984). Pass design and redundant strains in forward tube extrusion, *Journal* of *Mechanical Working Technology*, Vol. 9, pp. 313–324.
13. Blazynski, T. Z. (1976). *Metal forming tool profiles and flow*. Macmillan, New York, pp. 337-339.
14. Chang, K. T. & Choi, J. C. (1972). Upper-bound solutions to tube extrusion problems through curved dies. *Journal of Engineering for Industry-Transactions of the ASME*, Vol. 94, pp. 1108–1112.